Influence of the ionic liquid presence on the selective oxidation of glucose over molybdenum based catalysts

C. Megías-Sayago [a,b,*], C.J. Carrasco [a], S. Ivanova [a,b], F.J. Montilla [a], A. Galindo [a], J.A. Odriozola [a,b]

[a] Departamento de Química Inorgánica, Universidad de Sevilla, C/ Profesor García González, S/N, 41012, Sevilla, Spain

[b] Instituto de Ciencia de Materiales de Sevilla, Centro mixto CSIC-US, Avda. Américo Vespucio 49, 41092, Sevilla, Spain

*Corresponding author: cristina.megias@icmse.csic.es

Abstract

Two different approaches are proposed in this work in order to study the influence of the ionic liquid presence in the reaction of glucose oxidation by H_2O_2 in mild conditions. The ionic liquids are applied either as a solvent by using homogeneous Mo based catalyst, $[Mo(O)(O_2)_2(H_2O)_n]$ complex, or by using it as an integral part of an heterogeneous catalyst, organic inorganic hybrids based on Mo Keggin structure. Both catalytic strategies resulted in acceptable glucose transformation degrees but lead to different oxidation products depending on the role of the ionic liquid. The hybrid approach restrains the number of the received products being the most selective one. A detailed study of the effect of the hybrid nature and reaction conditions is proposed in the second part of this study.

Keywords: glucose oxidation, ionic liquids, molybdenum catalysts, polioxometalates

1. Introduction

The efficient transformations of polysaccharides into valuable compounds, such as fuels and important intermediate chemicals is a relevant topic nowadays and has attracted the attention of the scientific community [1–4]. The glucose, the monomer of cellulose, constitutes the most abundant and available monosaccharide and its transformations into furan derivatives like HMF (hydroxymethyl furfural) [5], FDCA (Furan dicarboxylic acid) [6], DFF (2,5 diformylfuran) [7] or sugar acids (aldonic and aldaric acids) is being widely investigated in the last years [8–10]. Within added-value chemicals issued from glucose, the gluconic acid, obtained via oxidation of the glucose aldehyde group is in versatile use in pharmaceutical, chemical, food, beverage and textile industries, either as additive, as chelating agent for cleaning purposes or for the extraction of metal traces in solutions [11]. Its current production is carried out via enzymatic process, in presence of glucose oxidase. However, this methods presents several drawbacks such as need of high amounts of expensive enzyme, its irreversible deactivation, the exhaustive control of process parameters (such as pH and temperature), the need of several pre-reaction purification processes in order to remove impurities and the long reaction times to obtain acceptable yields [12]. All this disadvantages stimulates the pursuit for new efficient, environmental friendly catalysts and processes to improve carbohydrate conversion and, therefore, biomass exploitation.

The production of gluconic acid has been studied over catalysts of different nature, including enzymatic [13] and heterogeneous, based on platinum [14,15] and, more recently, on gold [16,17]. Recently, a group of compounds, the as called ionic liquids (ILs), showed great potential in carbohydrate chemistry either as catalyst or as a solvent. The ILs are compounds consisting in ions with melting points below 100 ºC whose

principal advantages could be resumed in high ionic mobility, good electric conductivity, low vapor pressure and good thermal and chemical stability [18,19]. Most commonly used ILs are composed by quaternary ammonium salts or cyclic amine salts [20]. They have already found its application in catalysis as a solvents [21–24] in electrochemistry [25] and organic synthesis, however, the use of the ionic liquid as a part of hybrid catalyst is barely studied [20,26–30].

On the other hand the polyoxometalates, well-known catalytically active compounds were also considered as a potential glucose transformation catalysts [20]. In particular, the Keggin-type polyoxometalates, classified as anionic metal-oxygen clusters of the early transition metals, appear as a good candidates for carbohydrate conversion [31–33]. Properties like strong Brönsted acidity, fast multi-electron transfer, high proton mobility, high solubility in various solvents and resistance to hydrolytic and oxidative degradations in solutions converts these compounds in versatile materials for using in catalysis [34]. Furthermore, their properties can be tuned by varying the composition and the counter cations [31,35,36]. The proton compensated polyoxometalates, known as heteropoly acids (HPA) however cannot be used in liquid-phase reactions with polar solvents due to their solubility and impossibility for recuperation. However, the substitution of protons with another organic or inorganic cations results in insoluble materials and, therefore, useful in heterogeneously catalyzed liquid-phase reactions [31]. Additionally, the substitution of all the protons with organic cations could results in a new class of organic-inorganic hybrid materials which takes advantages on both inorganic (strength, thermal stability and chemical resistance) and organic part (lightness, flexibility and versatility) features. Perfect example of organic cations which could be applied in the hybrid are those of ionic liquids (ILs) [20,37–39].

In this context, the main goal of this work is to study the influence of the IL on the

catalytic performance of Mo based compounds. The ionic liquids are evaluated either as a solvent (*System 1*) or as integral part of the catalyst (*System 2*) in the liquid-phase oxidation of glucose with hydrogen peroxide as oxidant. In *system 1*, 1-butyl-3-methylimidazolium hexafluorophosphate (Bmim)PF_6 ionic liquid is used as solvent and $[Mo(O)(O_2)_2(H_2O)_n]$ complex as catalyst. In *system 2*, three different hybrids based on phosphomolybdic acid ($PMo_{12}O_{40}^{3-}$) and three IL cations, 1-ethyl-3-methylimidazolium (Emim), 1-buthyl-3-methylimidazolium (Bmim) and 1-hexyl-3-methylimidazolium (Hexmim), are used as catalysts in aqueous solution.

2. Experimental

2.1 Synthesis

Synthesis of oxodiperoxomolybdenum complex *(System 1)*

Solution of the aqua complex of oxodiperoxomolybdenum, $[Mo(O)(O_2)_2(H_2O)_n]$ (henceforth $[MoO_5]$) was prepared as follows. A suspension of MoO_3 (Sigma Aldrich, 3.617 g, 25 mmol) in 40 mL 30% aqueous hydrogen peroxide (VWR) was heated at 50 ºC with continuous stirring overnight after which complete dissolution of the molybdenum resulting in a clear yellow solution was observed. At this point the solution was cooled to 0 ºC and several drops of hydrogen peroxide were added and the solution was then made up to 100 mL and stored in a sealed volumetric flask at 4 ºC. Occasional venting of this solution is advised upon prolonged storage due to the accumulation of pressure following catalytic decomposition of hydrogen peroxide. A solution of $[MoO_5]$ with concentration 0.25 M is thus obtained.

Synthesis of heteropolyacid and hybrids *(System 2)*

Phosphomolybdic acid was prepared as reported in the literature [40] by using $Na_2MoO_4.2H_2O$ (Sigma Aldrich), H_3PO_4 (85%) (Panreac), HCl (37%) (VWR), diethyl ether (Panreac), HNO_3 (65%) (VWR) and distilled water.

For the $Emim_3[PMo_{12}O_{40}]$ (from this point forward Emim-Mo) synthesis [30], appropriate quantities of prepared $H_3PMo_{12}O_{40}$ (0.9 g) and 1-ethyl-3-methylimidazolium methanesulfonate (Alfa Aesar) were dissolved in distilled water (20 mL) separately. When mixed, a precipitate was formed, then filtered and dried at room temperature. Another two hybrids were analogously prepared by using 1-butyl-3-methylimidazolium methanesulfonate (Sigma Aldrich) to produce the $Bmim_3[PMo_{12}O_{40}]$ (Bmim-Mo) and 1-hexyl-3-methylimidazolium chloride (Alfa Aesar) for $Hexmim_3[PMo_{12}O_{40}]$ (Hexmim-Mo). All the hybrids were used as prepared and their structures are presented in Figure 1.

Figure 1. Structure of IL/ $PMo_{12}O_{40}$ hybrids used as catalytic *System 2.*

2.2 Characterization

X-ray diffraction (XRD) analysis were registered on a Panalitycal X'Pert Pro diffractometer, equipped with Cu anode with 0,05° step size and time acquisition of 80 s at room temperature in the 5-65 º2θ range.

Temperature dependent X-ray diffraction (TDRX) analysis was performed in a high temperature camera Anton Paar HTK 1200 coupled with an X'Pert Pro Philips diffractometer equipped with Cu anode. The diffractograms were taken every 50°C in the range of 30–750°C, from 5° to 65° 2θ (step size 0,05º and step time 50 s) in air. The heating ramp was fixed to 10°C/min.

Raman spectroscopy analysis were performed in a LabRAM Horiba Jobin Yvon microscope equipped with confocal microscopy and green laser (λ=532 nm). Samples were studied with 50x lens and intensity filter (D2).

2.3 Catalytic reaction

General procedure for *System 1*

The reactor (a 50 mL vial equipped with a Young valve and containing a stirrer flea) was charged with 0.25 M aqueous [MoO_5] (100 µL, 2.5 mol% of glucose), the solvent [41] (BmimPF$_6$, 2 mL), the oxidant (30 % aqueous H_2O_2, 340 µL, 3 mmol) and α-D-Glucose (Sigma Aldrich, 182 mg, 1 mmol), in the aforementioned order. The reactor was sealed and the solution reacted with constant stirring (600 rpm) in a thermostated oil bath (60 $^\circ$C) during 18 hours. Upon completion, the reactor was immediately cooled to 0 ºC and the mixture was extracted with H_2O (3 × 2 ml) and filtered with 0.45 µm nylon syringe filter. The resulting solution was diluted in ultra-pure water (500 μL of sample + 500 μL of H_2O) and analyzed by HPLC by using a Hi-Plex H column (300 x 7.7 mm), a refractive index detector (Varian 360-LC) and MilliQ water as mobile phase. Conversion, selectivity and C balance were obtained from HPLC measurements.

General procedure for *System 2*

α-D-Glucose (1 mmol) and 30 % hydrogen peroxide (3 mmol) were added to the reactor using water (2 mL) as solvent and each hybrid (0.25 or 2.5 mol% of glucose) as catalyst, respectively, at the above mentioned reaction conditions. In this case, no extraction process was necessary. Samples were analyzed in the same manner by HPLC.

3. Results and discussion

3.1 Hybrids characterization

3.1.1 *X Ray diffraction study*

XRD patterns of the phosphomolybdic acid and its corresponding hybrids are presented in Fig. 2. The hybrid patterns are very similar to that of the parent acid. Nevertheless, a shift and some new diffractions are detected accounting for the presence of organic cation around the Keggin anion and the formation of a new structure. The changes of the XRD profiles appear to be related to the type of cation being the XRD profile of Emim-Mo more similar to the parent acid than Bmim-Mo and Hexmim-Mo, in a way that shorter the aliphatic chain, smaller the modification of the parent acid diffractogram. For the Hexmim-Mo hybrid even new diffraction lines appear at low 2θ angles indicating most probably the formation of an ordered structure.

Figure 2. XRDiffractograms of $H_3PMo_{12}O_{40} \cdot 13H_2O$ (JCPDS #01-075-1588) and its hybrids.

3.1.2 *X-ray diffraction study as a function of temperature*

The phase transformations of the samples as a function of temperature are studied and presented. The XRD measurements are performed in flowing air from 30°C to 750°C with isotherms at every 50°C. However, Figure 3 presents only the temperatures for which significant changes are detected. The parent acid $H_3PMo_{12}O_{40} \cdot 13H_2O$ (JCPDS #01-075-1588) loses hydration water and transforms to $H_3PMo_{12}O_{40} \cdot 6H_2O$ (JCPDS#01-070-1705) and $H_3PMo_{12}O_{40} \cdot 1.5\ H_2O$ (JCPDS#00-046-0482) at 100 and 150 °C,

respectively. This phase remains intact till 450 ℃ where transforms into MoP_2O_7 (JCPDS#00-039-0026) and MoO_3 (JCPDS #00-001-0706 + #00-047-1081). From 550℃ till the last measured temperature only MoO_3 is detected.

The phase transformations of the hybrids seem to depend on the cation nature. Longer the substituted aliphatic chains of the imidazolium ring (ethyl through butyl to hexyl) lower the temperature of the first transformation. In addition, the transition of the hybrid structure to the decomposition products of the parent acid is always accompanied by samples amorphization. Emim-Mo is no longer available at temperatures higher than 300 ℃ and converts into MoO_3 at 500 ℃. Bmim-Mo is not observed at temperatures higher than 200 ℃, and instead, products issued from the decomposition of phosphomolybdic acid are detected with increasing of the temperature: $H_3PMo_{12}O_{40} \cdot 13H_2O$ (JCPDS #01-075-1588), $10MoO_3 \cdot H_3PO_4 \cdot 24H_2O$ (JCPDS #00-001-0032), MoP_2O_7 (JCPDS #00-039-0020) and MoO_3 (JCPDS #00-001-0706, #00-047-1081). Similar to Emim-Mo, at 500 ℃ only MoO_3 is detected. Hexmim-Mo is observed till 200 ℃ then an amorphization occurs and directly the MoO_3 appears at 550℃. In all the cases a MoO_3 crystallizes as a monocrystal, indicating a probable structure directing role of the imidazolium cations.

Figure 3. XRDiffractograms as a function of temperature: A) $H_3PMo_{12}O_{40} \cdot 13H_2O$, B) Emim-Mo, C) Bmim-Mo and D) Hexmim-Mo

All identified phases for the three hybrids and parent phosphomolybdic acid at every studied temperature are summarized in Table 1. The dependence of the hybrid's stability on the organic counter cation could be easily observed. Emim-Mo hybrid is the most stable followed by Bmim-Mo and Hexmim-Mo hybrids. A possible relationship

could be envisaged, less perturbation of the Keggin-structure higher phase transformation stability.

Table 1. Identified crystal phases at different temperatures

Temperature, ºC	Phases (H₃PMo₁₂O₄₀·13H₂O)	Phases (Emim₃[PMo₁₂O₄₀])	Phases (Bmim₃[PMo₁₂O₄₀])	Phases (Hexmim₃[PMo₁₂O₄₀])
RT	$H_3PMo_{12}O_{40} \cdot 13H_2O$	$Emim_3[PMo_{12}O_{40}]$	$Bmim_3[PMo_{12}O_{40}]$	$Hexmim_3[PMo_{12}O_{40}]$
50	$H_3PMo_{12}O_{40} \cdot 13H_2O$	$Emim_3[PMo_{12}O_{40}]$	$Bmim_3[PMo_{12}O_{40}]$	$Hexmim_3[PMo_{12}O_{40}]$
100	$H_3PMo_{12}O_{40} \cdot 6H_2O$	$Emim_3[PMo_{12}O_{40}]$	$Bmim_3[PMo_{12}O_{40}]$	$Hexmim_3[PMo_{12}O_{40}]$
150	$H_3PMo_{12}O_{40} \cdot 1.5H_2O$	$Emim_3[PMo_{12}O_{40}]$	$Bmim_3[PMo_{12}O_{40}]$	$Hexmim_3[PMo_{12}O_{40}]$
200	$H_3PMo_{12}O_{40} \cdot 1.5H_2O$	$Emim_3[PMo_{12}O_{40}]$	$Bmim_3[PMo_{12}O_{40}]$	$Hexmim_3[PMo_{12}O_{40}]$
250	$H_3PMo_{12}O_{40} \cdot 1.5H_2O$	$Emim_3[PMo_{12}O_{40}]$	$H_3PMo_{12}O_{40} \cdot 13H_2O$ + $10MoO_3 \cdot H_3PO_4 \cdot 24H_2O$	Amorphous
300	$H_3PMo_{12}O_{40} \cdot 1.5H_2O$	$Emim_3[PMo_{12}O_{40}]$	$H_3PMo_{12}O_{40} \cdot 13H_2O$ + $10MoO_3 \cdot H_3PO_4 \cdot 24H_2O$	Amorphous
350	$H_3PMo_{12}O_{40} \cdot 1.5H_2O$	$H_3PMo_{12}O_{40} \cdot 13H_2O$ + $10MoO_3 \cdot H_3PO_4 \cdot 24H_2O$	$H_3PMo_{12}O_{40} \cdot 13H_2O$ + $10MoO_3 \cdot H_3PO_4 \cdot 24H_2O$	Amorphous
400	$H_3PMo_{12}O_{40} \cdot 1.5H_2O$	$H_3PMo_{12}O_{40} \cdot 13H_2O$ + $10MoO_3 \cdot H_3PO_4 \cdot 24H_2O$ + MoP_2O_7	$H_3PMo_{12}O_{40} \cdot 13H_2O$ + $10MoO_3 \cdot H_3PO_4 \cdot 24H_2O$ + MoP_2O_7	Amorphous
450	MoP_2O_7 + MoO_3	$H_3PMo_{12}O_{40}$ + MoP_2O_7 + MoO_3	$10MoO_3 \cdot H_3PO_4 \cdot 24H_2O$ + MoP_2O_7	Amorphous
500	MoP_2O_7 + MoO_3	MoO_3	MoO_3	Amorphous + MoO_3
550	MoO_3	MoO_3	MoO_3	MoO_3
600	MoO_3	MoO_3	MoO_3	MoO_3
650	MoO_3	MoO_3	MoO_3	MoO_3
700	MoO_3	MoO_3	MoO_3	MoO_3
750	MoO_3	MoO_3	MoO_3	MoO_3

3.1.3 *Raman Spectroscopy*

The XRD studies demonstrate the structural similarity of the hybrids to the parent acid and the changes induced by the aliphatic chain of the substituted imidazolium ring. These changes are also studied by Raman spectroscopy (Fig. 4). The Keggin structural units presents four types of oxygen [42]: terminal oxygen, Ot (Mo═O), two types of bridging oxygen atoms (Mo─O─Mo), edge sharing oxygen Oe and corner sharing oxygen Ob, as well as corner sharing oxygen atoms between the central heteroatom and surrounding metal atoms Oa (P─O─Mo(x3)). Therefore, four oxygen bonds can be distinguished. The Raman spectra of the hybrids can be separated in two vibrational zones: the first one, within 100 - 1100 cm^{-1} metal-oxygen bonds range, (Fig. 4A) and the second one corresponding to organic fraction vibrations, in the 2700 - 3200 cm^{-1} range (Fig. 4B). The bands attribution and its comparison with literature data are presented in table 2.

Figure 4. Raman spectra of $H_3PMo_{12}O_{40} \cdot 13H_2O$ and hybrids

In general, the vibrational bands assigned to the metal-oxygen bonds do not change significantly in the presence of different imidazolium derivatives, the Keggin unit seems preserved, as confirmed by XRD. The Mo─Ob─Mo and Mo─Oe─Mo bands are slightly shifted for the hybrids: indicating that the organic cations situates near the bridging oxygens thus affecting their electronic density and causing the blue shift.

For all the hybrids the CH vibration are present confirming the formation of the hybrids together with the preservation of the Keggin structural unit.

Table 2. Vibrational assignments for inorganic and organic fractions

Experimental Raman shift, cm^{-1}	Raman shift, cm^{-1} [43,44]	Assignment	Experimental Raman shift, cm^{-1} [45–48]	Assignment [a]
993	995[43]	ν_s (Mo=Ot)	2835	ν_s CH-CH (imidazolium)
969	981[43]	ν_{as} (Mo=Ot)	2876	ν_s CH R$_2$
904,878	909-876 [44]	ν_{as} (Mo-Ob-Mo)	2919	ν_s CH R$_1$
602	603[44]	ν_s (Mo-Oe-Mo)	2940	CH$_3$NHCH
245, 222	251[44]	ν_s (Mo-Oa)	2968	ν_{as} CH R$_1$
			3018	ν_{as} CH R$_2$
			3107	NC(H)N
			3170	ν_{as} CH-CH (imidazolium)

[a] R$_1$ (ethyl, butyl or hexyl), R$_2$ (methyl)

3.2 Catalytic performance

The oxidation of glucose was carried out following the procedure described above for the two systems. The obtained results for *System 1* are shown in Fig. 5, as glucose conversion and yield in presence or absence of [MoO$_5$]. As could be expected, BmimPF$_6$ plays an important role when used as reaction media, a glucose conversion of 60 % is observed (Fig. 5A) in absence of catalyst, which suggests the participation of the ionic liquid not only as a solvent but also as a catalyst. The conversion surprisingly

drops in presence of the catalyst [MoO$_5$] to 41 % of conversion. As for the products (Fig. 5B), both reactions result in the same oxidation products, being gluconic acid the main product. Thus, higher yields are observed in absence of catalyst (35 % of yield *vs.* 27 % in presence of [MoO$_5$]) in the same way for glucaric acid (17 % of yield *vs.* 13 % in presence of [MoO$_5$]) and formic acid (7 % in absence of [MoO$_5$] *vs.* 1.6 %). A C balance of 100 % is obtained in presence of [MoO$_5$] and only 89 % balanced when IL is used. These results suggest that, although a lower conversion obtained in presence of [MoO$_5$] the oxidation reactions to glucaric and gluconic acids are promoted and the total degradation of glucose to formic acid suppressed. On the other hand the deficiency of the C balance in the case of the IL catalyzed reaction suggests additional products formation, either probably resulting from polymerization reactions or not extracted in the aqueous phase, and not detected by our HPLC method.

Figure 5. Glucose conversion (%) A) and product yield (%) B) with IL as a solvent Reaction conditions: 1 mmol of glucose, 3 mmol of H$_2$O$_2$, [MoO$_5$] (2.5 mol% of glucose), 2 mL of BmimPF$_6$, 600 rpm, 60 ºC, 18 hours.

The obtained results for *System 2* are presented in Fig. 6, in presence or absence of the hybrid Bmim-Mo catalyst. Approximately a 21 % of conversion is obtained in absence of catalyst, and corresponds to the formation of gluconic acid (glucaric acid traces are also observed). This result changes in presence of Bmim-Mo, where the conversion of glucose doubles to 40 % with 100 % selectivity to gluconic acid. The presence of Bmim-Mo catalyst inhibits the glucose oxidation to glucaric acid. However, in the same way that for *System 1*, a C balance of 78% is reached which suggests the formation of polymerization products, as the most probable cause for C lost.

Figure 6. Glucose conversion (%) A) and product yield (%) B) for $Bmim_3[PMo_{12}O_{40}]$ catalyst. Reaction conditions: 1 mmol of glucose, 3 mmol of H_2O_2, catalyst (2.5 mol% of glucose), 2 mL of H_2O, 600 rpm, 60 ℃, 18 hours.

When comparing both systems (*System 1 vs. 2*) higher selectivity and yield to gluconic acid is observed when the IL hybrid is used as catalyst, suppressing the degradation of glucose to formic acid and the formation of glucaric acid as secondary oxidation product. The higher conversion observed for the *System 1* could be attributed only to higher IL/Glucose ratio, when IL is used as solvent/co-catalyst. At this point the *System 1* was abandoned due to the lowest selectivity in terms of number of formed products and only the hybrid materials are used for more detailed study. All oxidation products obtained in both systems are summarized in Fig. 7.

Figure 7. Oxidation products over *System 1* and *System 2*.

The influence of the amount of catalyst was studied by reducing ten times the quantity of catalyst (0.25 mol%), with the same reaction conditions described above. In addition, to find out how the ILs nature affects the reaction parameters, the Emim-Mo, Bmim-Mo and Hexmim-Mo hybrids are prepared and reacted. The obtained results are presented in Fig. 8.

Figure 8. Glucose conversion (%) and product yield (%) as a function of the catalyst's amount and the ILs nature.

It seems that the organic cation nature is hardly important in terms of glucose conversion. Nevertheless the conversion slightly increases with the amount of catalyst, as we could expect, obtaining a 100 % of selectivity to gluconic acid in all cases. Regarding the C balance, a 100 % is obtained when the used catalyst is 0.25mol% of glucose while about only 80 % when the amount of catalyst is ten times higher.

In order to evaluate the influence of the reaction time, the conversion and product distribution were also studied as a function of the time over Emim-Mo_0,25mol% (Emim$_3$[PMo$_{12}$O$_{40}$]; 0.25mol% of glucose amount) catalyst (Fig. 9.).

Figure 9. Glucose conversion (%) A) and yield (%) B) over Emim-Mo_0.25mol% catalyst as a function of reaction time

The glucose conversion remains practically unaltered with the reaction time obtaining a 25 % of conversion after 1 hour of reaction and only 30 % after 18 hours. However, 100 % of gluconic acid is reached at every point.

The results described above suggest that the IL/Keggin hybrid appears as a very selective catalyst for glucose oxidation. As the different organic fractions seem not to influence the conversion, an increase of that could be reached by the change of the Keggin part hybrid nature. Three different anions were used to obtain the hybrids with the following molecular formula Emim$_3$[PMo$_{12}$O$_{40}$], Emim$_3$[PMo$_{10}$V$_2$O$_{40}$] [49] and Emim$_3$[PW$_{12}$O$_{40}$] [30,40], respectively. In the same way, catalysts were used in a 0.25mol% and 2.5mol% of glucose. The results are presented in Figure 10.

Figure 10. Glucose conversion (%) A) and products yield (%) B) as a function of the catalyst's amount and the Keggin anions nature.

The glucose conversion is slightly higher for the Mo-V containing Keggin anion hybrid while no significant differences between the two monoatomic (Mo, W) compounds are detected. The conversion increases with the amount of used catalyst except for Emim$_3$[PW$_{12}$O$_{40}$] which is the less active one. Regarding the product selectivity, 100 % of gluconic acid is obtained for the two monoatomic hybrids whereas formic acid is also detected in the case of Emim$_3$[PMo$_{10}$V$_2$O$_{40}$]. It seems that the introduction of heteroatoms, like V, in the Keggin organization promotes the oxidation and total degradation of glucose although the main product is still the desired gluconic acid. In fact, higher amount of catalyst leads to more gluconic acid yield in detriment to formic acid (10 % of yield *vs.* 5 % when 2.5 mol% is used).

All the studied hybrids present ability to catalyze the oxidation of glucose. However the products diversity should be controlled by the change of the Keggin heteroatoms or by the adjustment of the reaction parameters in order to increase the selectivity towards the gluconic acid formation.

4. Conclusions

Two different glucose conversion routes are proposed in this study: the direct transformation giving formic acid as a product and the oxidation reaction with gluconic and glucaric acid as products. The bare ionic liquid used as a solvent in *System 1* appears to catalyze both the glucose transformation into formic acid and the oxidation of the two terminal carbons, respectively. When combined with [Mo(O)(O$_2$)$_2$(H$_2$O)$_n$] catalyst, the direct transformation route is suppressed to some degree promoting the oxidation to aldonic and aldaric acids. The second approach using the ionic liquid/Keggin structure hybrids as catalytic *System 2* results in total selectivity to

15

gluconic acid and the disappearing of the direct transformation route. Conversion can be increased at higher catalyst charge without modifications in the selectivity. The changes in the ionic liquid nature result in a little variation of conversion, being the long chain hybrid the less active. On the other hand the changes of the Keggin structure affects the number of the obtained products suggesting that this change together with the reaction parameters readjustment could result in interesting modifications of the selectivity.

5. Acknowledgements

6. References

[1]   M.J. Climent, A. Corma, S. Iborra, Converting carbohydrates to bulk chemicals and fine chemicals over heterogeneous catalysts, Green Chem. 13 (2011) 520. doi:10.1039/c0gc00639d.

[2]   J. Song, H. Fan, J. Ma, B. Han, Conversion of glucose and cellulose into value-added products in water and ionic liquids, Green Chem. 15 (2013) 2619–2635. doi:10.1039/C3GC41141A.

[3]   D.M. Alonso, J.Q. Bond, J. a. Dumesic, Catalytic conversion of biomass to biofuels, Green Chem. 12 (2010) 1493. doi:10.1039/c004654j.

[4]   J.P.M. Sanders, J.H. Clark, G.J. Harmsen, H.J. Heeres, J.J. Heijnen, S.R. a Kersten, et al., Process intensification in the future production of base chemicals from biomass, Chem. Eng. Process. Process Intensif. 51 (2012) 117–136.

doi:10.1016/j.cep.2011.08.007.

[5]   S. Hu, Z. Zhang, J. Song, Y. Zhou, B. Han, Efficient conversion of glucose into 5-hydroxymethylfurfural catalyzed by a common Lewis acid SnCl4 in an ionic liquid, Green Chem. 11 (2009) 1746. doi:10.1039/b914601f.

[6]   A. Jain, S.C. Jonnalagadda, K. V. Ramanujachary, A. Mugweru, Selective oxidation of 5-hydroxymethyl-2-furfural to furan-2,5-dicarboxylic acid over spinel mixed metal oxide catalyst, Catal. Commun. 58 (2015) 179–182. doi:10.1016/j.catcom.2014.09.017.

[7]   A.S. Amarasekara, D. Green, E. McMillan, Efficient oxidation of 5-hydroxymethylfurfural to 2,5-diformylfuran using Mn(III)-salen catalysts, Catal. Commun. 9 (2008) 286–288. doi:10.1016/j.catcom.2007.06.021.

[8]   S. Jia, Z. Xu, Z.C. Zhang, Catalytic conversion of glucose in dimethylsulfoxide/water binary mix with chromium trichloride: Role of water on the product distribution, Chem. Eng. J. 254 (2014) 333–339. doi:10.1016/j.cej.2014.05.121.

[9]   X. Tong, Y. Ma, Y. Li, Biomass into chemicals: Conversion of sugars to furan derivatives by catalytic processes, Appl. Catal. A Gen. 385 (2010) 1–13. doi:10.1016/j.apcata.2010.06.049.

[10]   D. Bin, H. Wang, J. Li, H. Wang, Z. Yin, J. Kang, et al., Controllable oxidation of glucose to gluconic acid and glucaric acid using an electrocatalytic reactor, Electrochim. Acta. 130 (2014) 170–178. doi:10.1016/j.electacta.2014.02.128.

[11]   S. Ramachandran, P. Fontanille, A. Pandey, C. Larroche, Gluconic Acid : Properties , Applications and Microbial Production, 44 (2006) 185–195.

[12]   K. Buchholz, J. Seibel, Industrial carbohydrate biotransformations, Carbohydr. Res. 343 (2008) 1966–1979. doi:10.1016/j.carres.2008.02.007.

[13]   S. Anastassiadis, H.J. Rehm, Continuous gluconic acid production by the yeast-like Aureobasidium pullulans in a cascading operation of two bioreactors, Appl. Microbiol. Biotechnol. 73 (2006) 541–548. doi:10.1007/s00253-006-0499-y.

[14]   M. Besson, F. Lahmer, P. Gallezot, P. Fuertes, G. Fléche, Catalytic Oxidation of Glucose on Bismuth-Promoted Palladium catalysts, J. Catal. 152 (1995) 116–121.

[15]   I. Nikov, K. Paev, Palladium on alumina catalyst for glucose oxidation: reaction kinetics and catalyst deactivation, Catal. Today. 24 (1995) 41–47. doi:10.1016/0920-5861(95)00011-4.

[16]   P. Beltrame, M. Comotti, C. Della Pina, M. Rossi, Aerobic oxidation of glucose, Appl. Catal. A Gen. 297 (2006) 1–7. doi:10.1016/j.apcata.2005.08.029.

[17]   U. Prüße, M. Herrmann, C. Baatz, N. Decker, Gold-catalyzed selective glucose oxidation at high glucose concentrations and oxygen partial pressures, Appl. Catal. A Gen. 406 (2011) 89–93. doi:10.1016/j.apcata.2011.08.013.

[18]   J.P. Hallett, T. Welton, Room-temperature ionic liquids: solvents for synthesis and catalysis. 2, Chem. Rev. 111 (2011) 3508–3576. doi:10.1021/cr1003248.

[19]   P. Wasserscheid, T. Welton, Ionic Liquids in Synthesis, Wiley-VCH, 2003.

[20]   S. Ivanova, Hybrid organic-inorganic materials based on polyoxometalates, ISRN Chem. Eng. 2014 (2014) Article ID 963792, 13 pages. doi:10.1155/2014/963792.

[21]   C. DeCastro, Immobilised Ionic Liquids as Lewis Acid Catalysts for the

Alkylation of Aromatic Compounds with Dodecene, J. Catal. 196 (2000) 86–94. doi:10.1006/jcat.2000.3004.

[22]   R.S. Avellaneda, S. Ivanova, O. Sanz, F. Romero-Sarria, M.A. Centeno, J.A. Odriozola, Ionic liquid templated TiO2 nanoparticles as a support in gold environmental catalysis, Appl. Catal. B Environ. 93 (2009) 140–148. doi:10.1016/j.apcatb.2009.09.023.

[23]   M. Herbert, F. Montilla, A. Galindo, R. Moyano, A. Pastor, E. Álvarez, Influence of N-donor bases and the solvent in oxodiperoxomolybdenum catalysed olefin epoxidation with hydrogen peroxide in ionic liquids., Dalton Trans. 40 (2011) 5210–5219. doi:10.1039/c1dt10065c.

[24]   M. Herbert, A. Galindo, F. Montilla, Catalytic epoxidation of cyclooctene using molybdenum(VI) compounds and urea-hydrogen peroxide in the ionic liquid [bmim]PF6, Catal. Commun. 8 (2007) 987–990. doi:10.1016/j.catcom.2006.10.008.

[25]   L. Zhang, Q. Zhang, J. Li, Electrochemical behaviors and spectral studies of ionic liquid (1-butyl-3-methylimidazolium tetrafluoroborate) based sol-gel electrode, J. Electroanal. Chem. 603 (2007) 243–248. doi:10.1016/j.jelechem.2007.02.021.

[26]   S. Ivanova, X. Nitsch, F. Romero-Sarria, B. Louis, M.A. Centeno, A.C. Roger, et al., Ionic liquid protected heteropoly acids for methanol dehydration, Catal. Today. 171 (2011) 236–241. doi:10.1016/j.cattod.2011.03.077.

[27]   Y. Leng, J. Wang, D. Zhu, X. Ren, H. Ge, L. Shen, Heteropolyanion-Based Ionic Liquids: Reaction-Induced Self-Separation Catalysts for Esterification, Angew. Chemie Int. Ed. 48 (2009) 168–171. doi:10.1002/anie.200803567.

[28]   H. Li, Y. Qiao, L. Hua, Z. Hou, B. Feng, Z. Pan, et al., Imidazolium

Polyoxometalate: An Ionic Liquid Catalyst for Esterification and Oxidative

Esterification, ChemCatChem. 2 (2010) 1165–1170.

doi:10.1002/cctc.201000021.

[29]   T. Rajkumar, G. Ranga Rao, Characterization of hybrid molecular material

prepared by 1-butyl 3-methyl imidazolium bromide and phosphotungstic acid,

Mater. Lett. 62 (2008) 4134–4136. doi:10.1016/j.matlet.2008.06.029.

[30]   G. Ranga Rao, T. Rajkumar, B. Varghese, Synthesis and characterization of 1-

butyl 3-methyl imidazolium phosphomolybdate molecular salt, Solid State Sci.

11 (2009) 36–42. doi:10.1016/j.solidstatesciences.2008.05.017.

[31]   W. Deng, Q. Zhang, Y. Wang, Polyoxometalates as efficient catalysts for

transformations of cellulose into platform chemicals, Dalt. Trans. 41 (2012)

9817. doi:10.1039/c2dt30637a.

[32]   D. An, A. Ye, W. Deng, Q. Zhang, Y. Wang, Selective Conversion of Cellobiose

and Cellulose into Gluconic Acid in Water in the Presence of Oxygen, Catalyzed

by Polyoxometalate-Supported Gold Nanoparticles, Chem. - A Eur. J. 18 (2012)

2938–2947. doi:10.1002/chem.201103262.

[33]   Y. Liu, L. Zhu, J. Tang, M. Liu, R. Cheng, C. Hu, One-pot, One-step Synthesis

of 2,5-Diformylfuran from Carbohydrates over Mo-Containing Keggin

Heteropolyacids, ChemSusChem. 7 (2014) 3541–3547.

doi:10.1002/cssc.201402468.

[34]   F. Cavani, Heteropolycompound-based catalysts: A blend of acid and oxidizing

properties, Catal. Today. 41 (1998) 73–86. doi:10.1016/S0920-5861(98)00039-

X.

[35]   N. Mizuno, M. Misono, Heterogeneous Catalysis, Chem. Rev. 98 (1998) 199–218. doi:10.1002/anie.201410738.

[36]   I. V. Kozhevnikov, Catalysis by heteropoly acids and multicomponent polyoxometalates in liquid-phase reactions, Chem. Rev. 98 (1998) 171–198. doi:10.1021/cr960400y.

[37]   X.X. Han, Y.F. He, C. Te Hung, L.L. Liu, S.J. Huang, S. Bin Liu, Efficient and reusable polyoxometalate-based sulfonated ionic liquid catalysts for palmitic acid esterification to biodiesel, Chem. Eng. Sci. 104 (2013) 64–72. doi:10.1016/j.ces.2013.08.059.

[38]   E. Rafiee, F. Mirnezami, Keggin-structured polyoxometalate-based ionic liquid salts: Thermoregulated catalysts for rapid oxidation of sulfur-based compounds using H2O2 and extractive oxidation desulfurization of sulfur-containing model oil, J. Mol. Liq. 199 (2014) 156–161. doi:10.1016/j.molliq.2014.08.036.

[39]   X. Han, W. Yan, K. Chen, C.-T. Hung, L.-L. Liu, P.-H. Wu, et al., Heteropolyacid-based ionic liquids as effective catalysts for the synthesis of benzaldehyde glycol acetal, Appl. Catal. A Gen. 485 (2014) 149–156. doi:10.1016/j.apcata.2014.08.001.

[40]   H. Wu, Contribution to the chemistry of phosphomolybdic acids, phosphotungstic acids, and allied substances., J. Biol. Chem. 43 (1920) 189–220.

[41]   S. Carda-Broch, A. Berthod, D.W. Armstrong, Solvent properties of the 1-butyl-3-methylimidazolium hexafluorophosphate ionic liquid, Anal Bioanal Chem. 375 (2003) 191–199.

[42]   S. Ganapathy, M. Fournier, J.F. Paul, L. Delevoye, M. Guelton, J.P. Amoureux, Location of protons in anhydrous keggin heteropolyacids H3PMo12O40 and

H3PW12O40 by 1H{31P}/31P{1H} REDOR NMR and DFT quantum chemical calculations, J. Am. Chem. Soc. 124 (2002) 7821–7828. doi:10.1021/ja017848n.

[43] J. Tatibou, A Two-Step Transformation of the Magnesium Salt of Phosphomolybdic Acid HMgPMo 12 O 40 Supported on Silica, 32 (1997) 22–32.

[44] C. Rocchiccioli-Deltcheff, A. Aouissi, M.M. Bettahar, S. Launay, M. Fournier, Catalysis by 12-Molybdophosphates, J. Catal. 164 (1996) 16–27.

[45] N.E. Heimer, R.E. Del Sesto, Z. Meng, J.S. Wilkes, W.R. Carper, Vibrational spectra of imidazolium tetrafluoroborate ionic liquids, J. Mol. Liq. 124 (2006) 84–95. doi:10.1016/j.molliq.2005.08.004.

[46] K.M. Dieter, C.J. Dymek, N.E. Heimer, J.W. Rovang, J.S. Wilkes, Ionic structure and interactions in 1-methyl-3-ethylimidazolium chloride-alcl3 molten-salts, J. Am. Chem. Soc. 110 (1988) 2722–2726. doi:10.1021/ja00217a004.

[47] E.R. Talaty, S. Raja, V.J. Storhaug, A. Dölle, W.R. Carper, Raman and Infrared Spectra and ab Initio Calculations of C 2 - 4 MIM Imidazolium Hexafluorophosphate Ionic Liquids, J. Phys. Chem. B. 108 (2004) 13177–13184. doi:10.1021/jp040199s.

[48] S. a Katsyuba, E.E. Zvereva, A. Vidis, P.J. Dyson, Application of density functional theory and vibrational spectroscopy toward the rational design of ionic liquids., J. Phys. Chem. A. 111 (2007) 352–370. doi:10.1021/jp064610i.

[49] Y. Leng, J. Wang, D. Zhu, L. Shen, P. Zhao, M. Zhang, Heteropolyanion-based ionic hybrid solid: A green bulk-type catalyst for hydroxylation of benzene with hydrogen peroxide, Chem. Eng. J. 173 (2011) 620–626. doi:10.1016/j.cej.2011.08.013.

Figure 1. Structure of IL/ $PMo_{12}O_{40}$ hybrids used as catalytic *System 2*.

Figure 2. XRDiffractograms of $H_3PMo_{12}O_{40} \cdot 13H_2O$ (JCPDS #01-075-1588) and its hybrids.

Figure 3. XRDiffractograms as a function of temperature: A) $H_3PMo_{12}O_{40} \cdot 13H_2O$, B) Emim-Mo, C) Bmim-Mo and D) Hexmim-Mo

Figure 4. Raman spectra of $H_3PMo_{12}O_{40} \cdot 13H_2O$ and hybrids

Figure 5. Glucose conversion (%) A) and product yield (%) B) with IL as a solvent Reaction conditions: 1 mmol of glucose, 3 mmol of H_2O_2, $[MoO_5]$ (2.5 mol% of glucose), 2 mL of $BmimPF_6$, 600 rpm, 60 ºC, 18 hours.

Figure 6. Glucose conversion (%) A) and product yield (%) B) for $Bmim_3[PMo_{12}O_{40}]$ catalyst. Reaction conditions: 1 mmol of glucose, 3 mmol of H_2O_2, catalyst (2.5 mol% of glucose), 2 mL of H_2O, 600 rpm, 60 ºC, 18 hours.

Figure 7. Oxidation products in *System 1* and *System 2*.

Figure 8. Glucose conversion (%) and product yield (%) as a function of the catalyst's amount and the ILs nature.

Figure 9. Glucose conversion (%) A) and yield (%) B) over Emim-Mo_0.25mol% catalyst as a function of reaction time.

Figure 10. Glucose conversion (%) A) and products yield (%) B) as a function of the catalyst's amount and the Keggin anions nature.
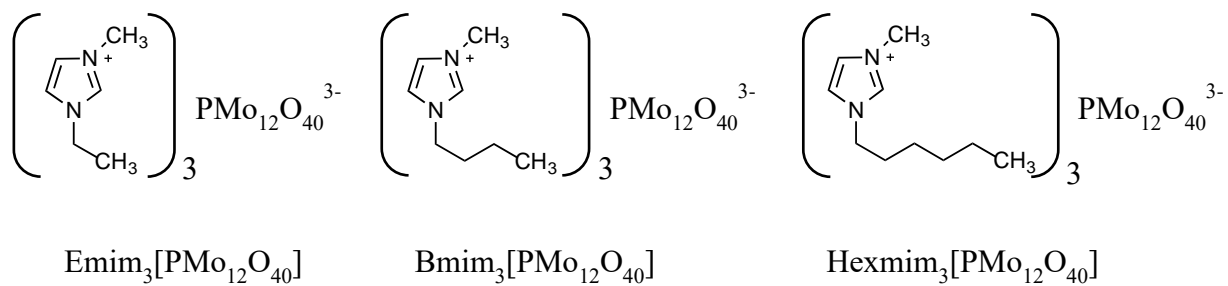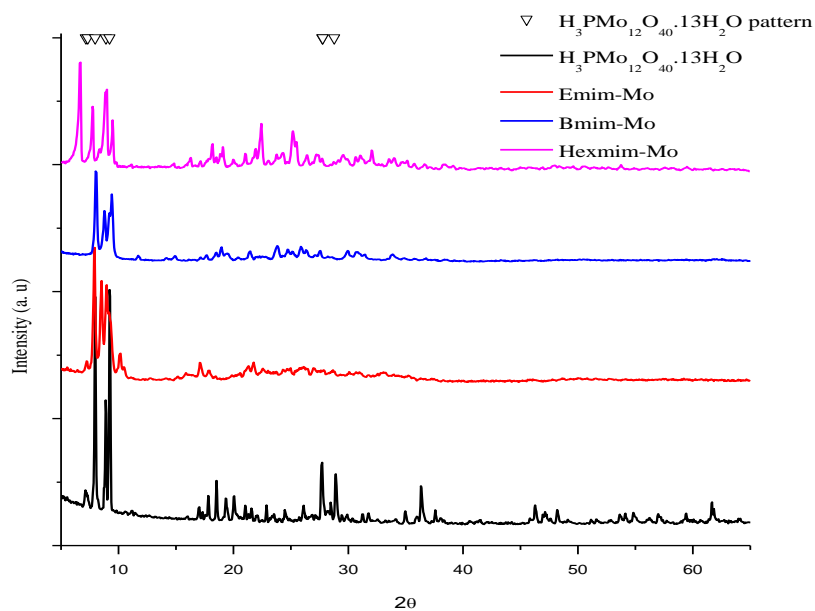
Figure 1

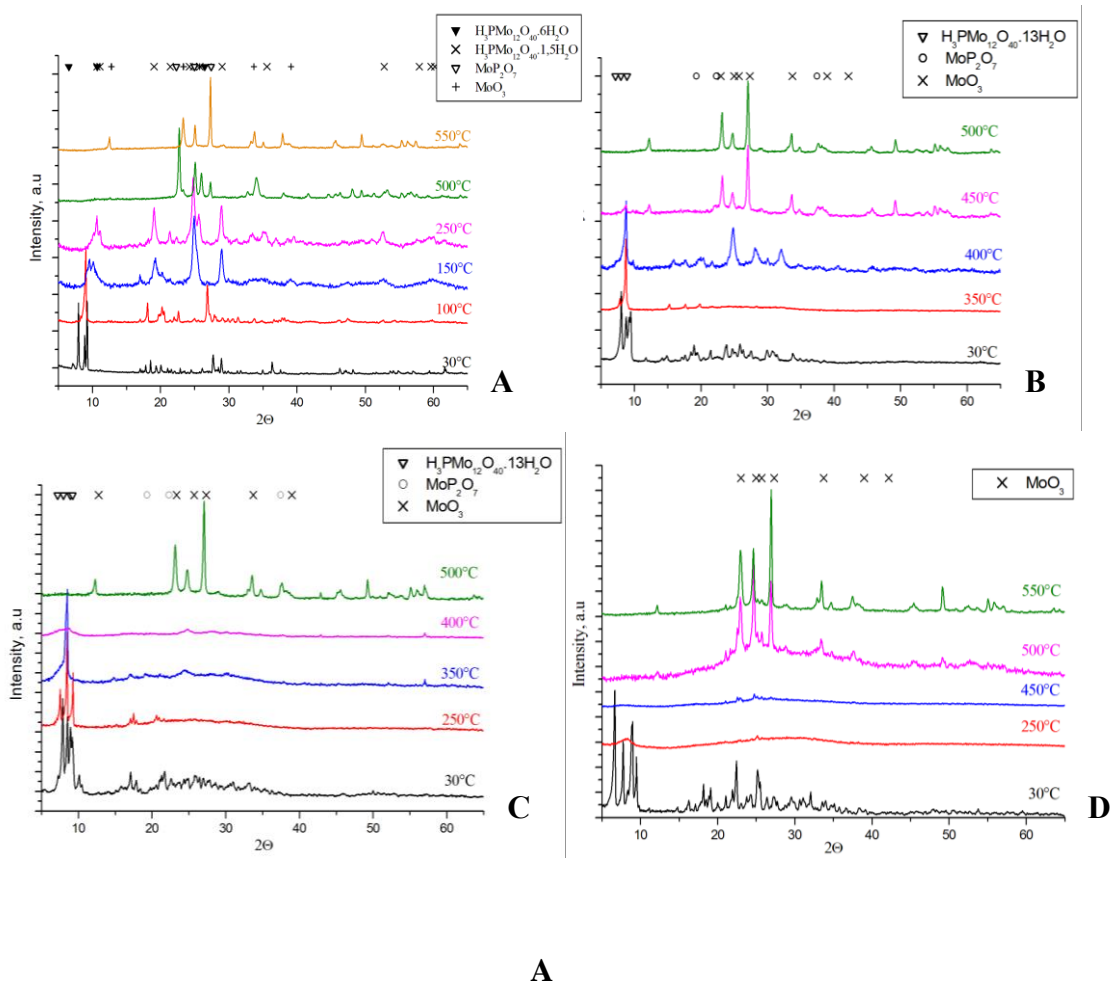$$\left(\text{Emim}^+ \right)_3 \text{PMo}_{12}\text{O}_{40}^{3-} \qquad \left(\text{Bmim}^+ \right)_3 \text{PMo}_{12}\text{O}_{40}^{3-} \qquad \left(\text{Hexmim}^+ \right)_3 \text{PMo}_{12}\text{O}_{40}^{3-}$$

$\text{Emim}_3[\text{PMo}_{12}\text{O}_{40}]$ $\qquad\qquad$ $\text{Bmim}_3[\text{PMo}_{12}\text{O}_{40}]$ $\qquad\qquad$ $\text{Hexmim}_3[\text{PMo}_{12}\text{O}_{40}]$

Figure 2

Figure 3

A
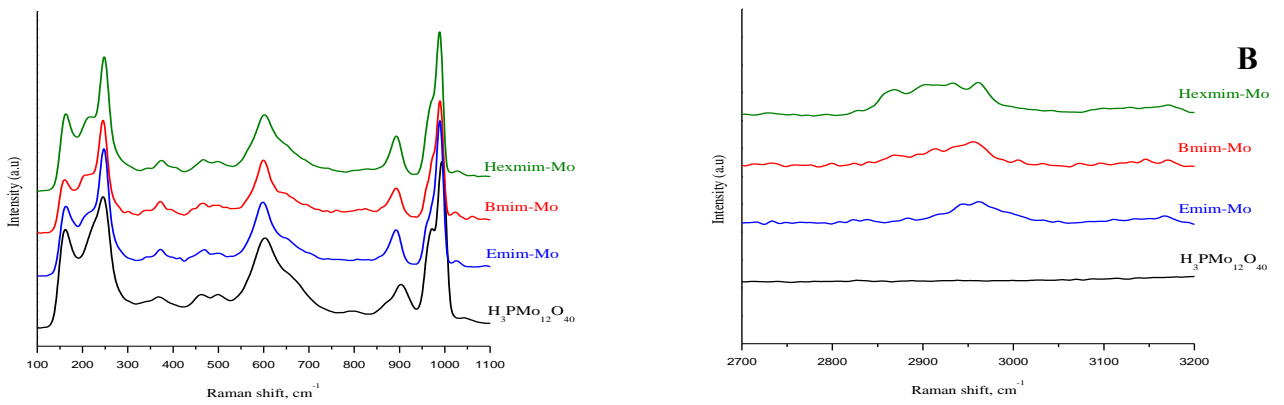
Figure 4

Figure 5

Figure 6

Figure 7

Gluconic acid	**Glucose**	**Formic acid**

Oxidation ← | Oxidation →

↓ Oxidation

Glucaric acid

Figure 8

■ Conversion (%)
■ Yield (%)

Figure 9

Figure 10

A

B